Aquacultural Engineering 109 (2025) 102509

Contents lists available at ScienceDirect

Aquacultural Engineering

journal homepage: www.elsevier.com/locate/aque

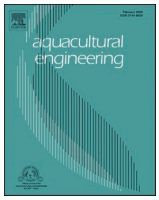

Towards understanding the dynamic behaviour of bioflocs in a fish tank culture: Integration of fish growth and activated sludge modelling

Nurhayati Br Tarigan [a,b,*], Marc Verdegem [b], Julie Ekasari [c], Karel J. Keesman [a,**]

[a] Mathematical and Statistical Methods - Biometris, Wageningen University and Research, Wageningen 6700AA, the Netherlands
[b] Aquaculture and Fisheries, Animal Sciences Group, Wageningen University and Research, Wageningen 6700 AH, the Netherlands
[c] Department of Aquaculture, Faculty of Fisheries and Marine Sciences, IPB University, Dramaga, Bogor, West Java 16128, Indonesia

ARTICLE INFO

Keywords:
Activated sludge model
Non-starch-polysaccharide
Nile tilapia
Biofloc
Nitrogen
Mathematical model

ABSTRACTS

Biofloc can improve the nutrient use efficiency of an aquaculture system. However, knowledge of the dynamic behaviour of biofloc related to the nutrient concentration in the water is limited. This study combined the fish growth model with the activated sludge model (ASM), later called fish-ASM, to understand the dynamic behaviour of biofloc in Nile tilapia culture. Fish were fed two types of diets that differ in fiber content. One of the diet contains three times higher fiber, which was formulated by incorporating more non-starch-polysaccharides (NSP). NSP is expected to increase carbon content in the water and promote more biofloc growth. Initial model parameter values were gained from experiments and ASM number 1. In fish-ASM, waste comes from uneaten feed, fish faeces, decay of heterotrophic and autotrophic biomass, and fish gill excretion (ammonia). Heterotrophic and autotrophic biomass then utilize the waste as substrates for their growth and part of the biomass is consumed by fish as natural food. The main model outputs in this study are hourly dynamics of fish, biofloc, and nitrogen in water. After trial and error calibration process, the model was fit to the fish, biofloc, and nitrogen dynamics of the lower fiber diet datasets with relative mean square error of 3 %-34 % to the corresponding average observations. However, future improvement was needed in the higher fiber diet simulation, especially related to biofloc and ammonia dynamics. The study shows that the development of biofloc was strongly influenced by organic matter availability.

1. Introduction

Inland aquaculture has been playing a crucial role in supplying animal protein, providing in 2022 74 % of the global production compared to 26 % produced in the marine environment (FAO, 2024). To minimize water and land use, aquaculture tends to intensify the system by increasing the stocking density which leads to a higher feed input per unit of aquaculture space (Verdegem et al., 2023). Although this strategy aims to increase fish production, it also increases waste production. Waste accumulation can eventually hamper fish growth and welfare due to poor water quality. Discharging the water without treatment will cause eutrophication of natural water bodies (Boyd et al., 2007). Hence, for sustainable development of aquaculture post or in-process treatment of the water is needed.

Biofloc technology (BFT) is a concept in aquaculture that utilizes microbiota to maintain water quality which enables a high-density culture with minimum water exchange. The main principle of BFT is to recycle nutrient waste into microbial biomass which can be later used as natural food for the culture animals (Avnimelech, 2009). Biofloc formation is mainly done by heterotrophic bacteria, and supported by algae and autotrophic bacteria (Ebeling et al., 2006). The growth of heterotrophs is stimulated by maintaining a high C/N ratio through direct addition of organic carbon in the water of by increasing the C/N ratio of the feed (Avnimelech, 2009; Bossier and Ekasari et al., 2017; Tinh et al., 2021; Vinasyiam et al., 2023). Hence, maintaining the C/N ratio is crucial in a biofloc system. On the one hand, insufficient amounts of carbon will inhibit biofloc formation and lead to poor water quality. On the other hand, carbon excess will lead to the accumulation of biofloc which eventually will hamper fish growth due to oxygen depletion and

Abbreviations: ASM, Activated sludge model; BFT, Biofloc technology; COD, Chemical oxygen demand; NSP, Non-starch pollysachharides; OM, Organic matter; RMSE, Relative mean square error; TAN, Total ammonia nitrogen.

* Corresponding author at: Mathematical and Statistical Methods - Biometris, Wageningen University and Research, Wageningen 6700AA, the Netherlands.
** Corresponding author.
E-mail addresses: nurhayati.brtarigan@wur.nl (N.B. Tarigan), karelkeesman@wur.nl (K.J. Keesman).

https://doi.org/10.1016/j.aquaeng.2024.102509
Received 29 September 2024; Received in revised form 17 December 2024; Accepted 18 December 2024
Available online 19 December 2024

Symbols

ADC_{OM}	Apparent digestibility coefficient of organic matter (-)
FCR_{Xba}, FCR_{Xbh}, FCR_{Xfeed}	Feed conversion ratio of autotrophic biomass, heterotrophic biomass, and pelleted feed, respectively (g dry weight g^{-1} fresh weight)
N_{Xba}, N_{Xbh}, N_{Xfeed}	Total nitrogen content of autotrophic biomass, heterotrophic biomass, and pelleted feed, respectively (g N kg^{-1})
q_{GXf}	Fish growth rate (g h^{-1})
q_{XfXnd}, q_{XfXs}, q_{XfSnh}	Waste production from fish in the form of nitrogen in faeces, organic matter in faeces, and ammonia, respectively (g h^{-1})
q_{XbaXf}, q_{XbhXf}, $q_{XfeedXf}$, q_{XNXf}	Uptake rate by fish of autotrophic biomass, heterotrophic biomass, pelleted feed, and total nitrogen, respectively (g h^{-1})
REN_{Xf}	Eaten nitrogen feed content retained in fish body (%)
S_{alk}	Alkalinity (Molar)
S_{co}	Carbon dioxide (g CO_2 m^{-3})
S_i	Soluble inert material (g COD m^{-3})
S_{nd}	Soluble organic nitrogen (g N m^{-3})
S_{nh}	Ammonia nitrogen (g N m^{-3})
S_{no}	Nitrite and nitrate nitrogen (g N m^{-3})
S_o	Oxygen (g O_2 m^{-3})
S_s	Soluble organic matter (g COD m^{-3})
X_{ba}	Autotrophic biomass (g COD m^{-3})
X_{bh}	Heterotrophic biomass (g COD m^{-3})
X_f	Fish (g COD m^{-3})
X_{feed}	Feed (g COD m^{-3})
X_i	Particulate inert material (g COD m^{-3})
X_{nd}	Particulate organic nitrogen (g COD m^{-3})
X_p	Non-degradable organic matter (g COD m^{-3})
X_{ph}	Phytoplankton (g COD m^{-3})
X_s	Particulate organic matter (g COD m^{-3})
μ	Average value of observation data

gill occlusion (Schveitzer et al., 2013).

Carbon can be introduced into the BFT system externally beside the feed or incorporated within the pelleted feed (Avnimelech, 2009; Bossier and Ekasari et al., 2017; Tinh et al., 2021; Vinasyiam et al., 2023). The latter has been done by the inclusion of non-starch polysaccharides (NSP) types of carbon into the diet (Kabir et al., 2020; Tarigan et al., 2025; Vinasyiam et al., 2023). Although there is a risk to lower fish production because a high dietary NSP content lowers the apparent digestibility of the feed, this diet-related approach can improve carbon use efficiency in a BFT system (Tarigan et al., 2025) and simplify carbon addition management (Vinasyiam et al., 2023).

To initiate optimum conditions for the growth of biofloc and fish, understanding the dynamic behaviour of biofloc is crucial. To date, knowledge of the dynamic behaviour of biofloc is still limited. Insight into different phenomena in a system can be obtained by mathematical models (Keesman, 2011), including aquaculture systems. Several models have been developed to understand the relationship between fish growth and nutrient dynamics in different aquaculture systems, including recirculated aquaculture system (RAS), ponds (Jiménez-Montealegre et al., 2002; Serpa et al., 2013; Svirezhev et al., 1984), and RAS-hydroponics systems (de Korte et al., 2024; Goddek et al., 2016; Tarigan et al., 2021). However, only a few studies incorporate biofloc in pond aquaculture models due to the complexity of biofloc behaviour. To date, models that incorporate biofloc in aquaculture systems viewed biofloc as one aggregated component, and the change of biofloc biomass was described by an exponential function based on experimental observations (Pinho et al., 2023; Tarigan et al., 2024). This is a considerable simplification because biofloc is an aggregate of different types of microbial biomass, has various functions, and is affected by environmental conditions, such as nutrient availability, temperature, and light (De Schryver et al., 2008).

The family of activated sludge models (ASM), starting with the work of Henze et al. (1987) and known as ASM No 1, has been widely used, for instance treat pharmaceutical waste (Li et al., 2023) and micro-pollutants (Mohammadi et al., 2022) or to improve nitrogen and bioplastic recovery (Ribeiro et al., 2022). ASM has been advanced significantly compared to the first published version (Daigger, 2011). In the family of ASM, micro-organisms play a crucial role in transforming slowly biodegradable into readily organic matter, converting the waste into microbial biomass, and converting ammonia nitrogen (TAN) into NO_3. The role of micro-organisms in activated sludge systems is similar to the role of biofloc in fish ponds, in which the waste comes from uneaten feed, faeces, and decaying organic matter (OM), the latter also including biofloc. The presence of cultured animals, e.g. Nile tilapia, in the BFT system enables fish to recycle part of the waste nutrients resulting from applying pelleted feed by consuming biofloc (De Schryver et al., 2008).

This study is the first to merge an activated sludge model (ASM) and a fish growth model to evaluate fish and biofloc formation in a biofloc system (fish-ASM). The aim of this study is to predict biofloc growth or decay, as well as organic and inorganic waste accumulation and utilization in a fish-biofloc systems. In this study, the fish-ASM model was developed studying Nile tilapia (*Oreochromis niloticus*) culture performance in lined biofloc rearing tanks, fed diets with either a low or high NSP content.

2. Methodology

2.1. System description

In this study, the dynamic behaviour of biofloc, fish, carbon, and nitrogen of a fish-biofloc system was simulated. The operational data was based on the experimental data of Tarigan et al. (2025). Fish, Nile tilapia juveniles, were cultivated in ten experimental lined tanks with a diameter of 2 m for 56 days at IPB University, Bogor, Indonesia. Water depth ranged between 0.55 and 0.85 m depending on daily precipitation, evaporation, and water replacement. Originally, the water level was intended to be maintained during the experiment by compensating for evaporation loss. However, this became unnecessary due to the high precipitation during the experiment, with a total rainfall of 832.9 mm. Instead, some water was discharged to avoid overflow in the tank due to precipitation, with a total water replacement of 6.0–6.4 m^3. Additionally, continuous aeration was applied to the rearing tank to maintain an oxygen level of at minimum 6 mg O_2/L. The initial body weight and stocking density of the fish were 17.3 ± 0.1 g and 15 fish/m^3, respectively. The feeding ration was around 16 g/$kg^{0.8}$/d and was administered equally twice a day, at 8.00 am and 4.00 pm. The average temperature during the culture period was 25 ± 2.5 ℃.

Two diets, differing in the type of carbon, were tested, assigning five replicate tanks per diet. One diet was mainly rich in starch (Control-diet) and the other was rich in NSP (High-NSP diet). Both diets had a similar protein content, around 29 % on dry matter basis. However, the High-NSP-diet contained 3 times more fiber compared to the Control-diet (13.3 % vs 4.3 % on dry matter basis). The NSP-rich ingredients in the High-NSP-diet mainly came from palm kernel meal, rice bran, and corn gluten feed, which are fibrous ingredients. The High-NSP-diet was expected to boost the biofloc growth because it reduces fish digestibility, hence providing more fiber-rich organic matter for the biofloc through

fish faeces (Tarigan et al., 2025; Vinasyiam et al., 2023).

2.2. Conceptual model

In principle, the model followed concepts of ASM No 1 (Henze et al., 1987) and combined it with the fish growth model of Tarigan et al. (2024).

Components in the model are expressed as S_j or X_j, in which the terms S and X represent soluble and particulate forms, respectively, and the subscript j represents different component names. Components included in this study were inert material (S_i and X_i), heterotrophic bacteria (X_{bh}), autotrophic bacteria (X_{ba}), phytoplankton (X_{ph}), organic matter (S_s and X_s), particulate matter arising from biofloc decay (X_p), organic nitrogen (S_{nd} and X_{nd}), ammonia nitrogen (S_{nh}), nitrite nitrogen (S_{no}), oxygen (S_o), alkalinity (S_{alk}), and carbon dioxide (S_{co}). The initial value of each component is shown in Table A.1. Components related to organic matter (S_i, X_i, X_{bh}, X_{ba}, S_s, X_s, and X_p) were expressed in g chemical oxygen demand (COD) per tank, nitrogen-related components (S_{nd}, X_{nd}, S_{nh}, S_{no}) were in g nitrogen (N) per tank, and S_o, S_{co}, and S_{alk} were in g O_2 per tank, g CO_2 per tank, and molar concentration per tank, respectively.

Organic waste in the fish tank refers to the sum of uneaten feed, fish faeces, decayed X_{bh}, and decayed X_{ba}. Preliminary results showed that the amount of decayed X_{ph} was almost negligible compared to the aforementioned organic waste. Similarly, the amount of active X_{ph} is also insignificant compared to other feed sources for the fish. Hence, it is excluded from the model calculation. Conversion from g feed and g fish to g COD was calculated from the protein, fat, and carbohydrate content (Davis et al., 2021). The processes driving conversions between model components are depicted in Fig. 1. S_i and X_i were not shown in the figure because these are inert materials, which means no conversion occurs during the cultivation period (Henze et al., 1987). The mass balance equation of each component of the model can be found in Table A.2, which in general is written as:

$$\text{Accumulation} = \text{Input} - \text{Output} + \text{Reaction} \quad (1)$$

In this fish-ASM, X_{bh} plays a crucial role in maintaining water quality through hydrolysis (conversion from X_s into S_s) and ammonification (conversion from S_{nd} into S_{nh}) process while through nitrification, ammonia nitrogen (S_{nh}) was converted into nitrite and nitrate nitrogen (S_{no}). X_{bh} can also reduce S_s and S_{nh} concentrations in water through uptake into X_{bh} biomass. The growth of X_{bh} and X_{ba} is dependent on S_s and S_{nh}, respectively. Additionally, their growth is associated with oxygen (S_o) utilization. In the case of anoxic conditions, the role of oxygen as a terminal electron acceptor in X_{bh} is replaced by nitrate (S_{no}). In other words, the growth of X_{bh} is affected by S_s and S_o in aerobic conditions and by S_s, S_o, and S_{no} in anoxic conditions. Compared to aerobic conditions, the hydrolysis rate of X_s into S_s is also lower under anoxic conditions. Additionally, part of X_{bh} and X_{ba} is grazed by fish, contributing to fish growth. Another part of the eaten X_{bh} and X_{ba} is excreted as faeces and ammonia, and kept in the nutrient cycle.

The organic waste (uneaten feed, fish faeces, and majority of decayed X_{bh} and X_{ba}) are associated with the activated sludge subsystem as particulate organic matter (X_s) which then is hydrolysed into soluble organic matter (S_s). The hydrolysis process rate is linear with X_{bh} concentration in the water. Additionally, a part of decayed X_{bh} and X_{ba} is converted into degradable particulate (X_p).

Besides organic matter, this study also examined nitrogen dynamics. The nitrogenous waste is divided into ammonia (S_{nh}), soluble organic nitrogen (S_{nd}), and particulate organic nitrogen (X_{nd}). Similar to X_s and S_s, the contributors of nitrogenous particulate organic waste (X_{nd}) are fish faeces, uneaten feed, and the majority of X_{bh} and X_{ba} decay. Inert nitrogenous material is neglected in the model because it is usually small. In parallel with the hydrolysis of organic waste, X_{nd} is hydrolysed into S_{nd}, which subsequently is partially converted into S_{nh}. Besides the ammonification process, the input of S_{nh} also comes from gill excretion.

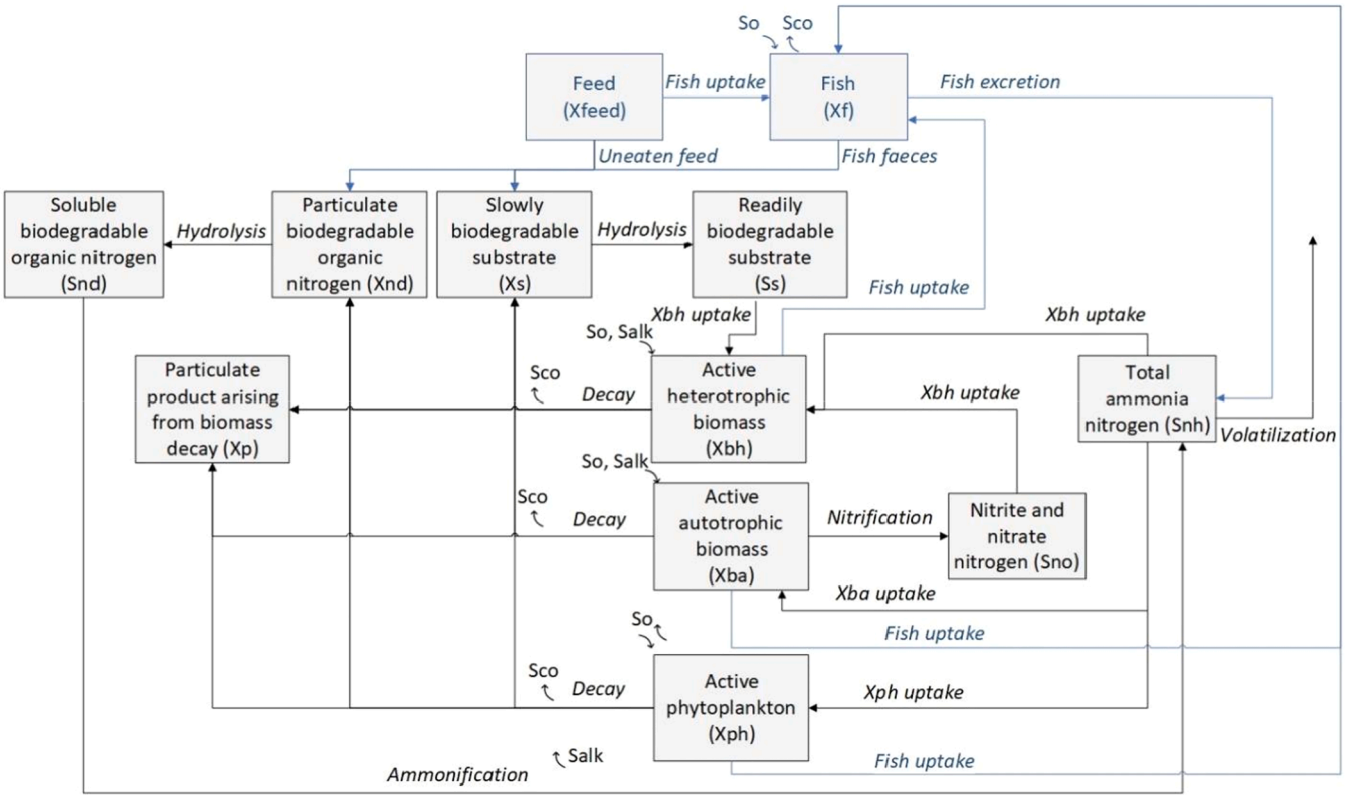

Fig. 1. Scheme of fish-ASM. S_{co}, S_o, and S_{alk} are carbon dioxide, oxygen, and alkalinity, respectively. Blue colour indicates components and processes related to the fish growth model.

2.3. Model equations

Mass balances expressing the dynamics or accumulation of each component are shown in Table A.2. Auxiliary equations of balance component (input, reaction, and output) in the mass balance are listed in Table A.3. Equations related to the ASM follow from Henze et al. (1987). Equations related to X_i and S_i are not shown because no reaction occurred in these components, they just enter the system through water inflow and leave through water replacement. Finally, parameter values used for the simulation can be found in Table A.4.

In terms of the contribution to X_s and X_{nd}, it was assumed that 5 % of the feed given is uneaten. X_{bh} and X_{ba} decay is proportional to each of their biomass in a first-order manner (Henze et al., 1987; Svirezhev et al., 1984). The term fish faeces (q_{XfXs}) was calculated based on the amount of eaten pelleted feed ($q_{XfeedXf}$), eaten X_{bh} (q_{XbhdXf}), eaten X_{ba} (q_{XbadXf}), and apparent digestibility coefficient of organic matter (ADC_{OM}), which can be written as:

$$q_{XfXs} = (1 - ADC_{OM}) * (q_{XfeedXf} + q_{XbhXf} + q_{XbaXf}) \quad (2)$$

Calculation of N content in fish faeces (q_{XfXnd}) is in line with q_{XfXs}, only the amount of eaten feed, X_{bh}, and X_{ba} is multiplied by each of their N content (N_{Xfeed}, N_{Xbh}, and N_{Xba}, respectively), and can be written as:

$$q_{XfXnd} = (1 - ADC_{OM}) * (N_{Xfeed} * q_{XfeedXf} + N_{Xbh} * q_{XbhXf} + N_{Xba} * q_{XbaXf}) \quad (3)$$

Finally, the contribution to S_{nh} from fish (q_{XfSnh}) was calculated based on total N consumed by fish from X_f, X_{bh}, and X_{ba} (q_{XNXf}) minus total N retained by fish body minus total N ended up as fish faeces, which can be written as:

$$q_{XfSnh} = q_{XNXf} - REN_{Xf}*q_{XNXf} - q_{XfXnd} \quad (4)$$

in which REN_{Xf} is the retention efficiency of N by the fish body and q_{XNXf} is defined as:

$$q_{XNXf} = N_{Xfeed}*q_{XfeedXf} + N_{Xbh}*q_{XbhXf} + N_{Xba}*q_{XbaXf} \quad (5)$$

In terms of reactions, in ASM these are expressed as multiplication between stoichiometric coefficients and process rate, which contains the kinetics parameters. Equations related to the reaction of each component are shown in Table A.3. Stoichiometric coefficients and process rate related to X_{bh} and X_{ba} growth and decay, ammonification, and hydrolysis of X_s and X_{nd} follow from ASM No 1 (Henze et al., 1987, see Table A.3 and A.4). Reactions related to fish growth follow from Tarigan et al. (2024). The fish uptake rate of X_{bh} and X_{ba} was assumed to be proportional to fish biomass and maximum uptake rate in a first order-manner, and to X_{bh} biomass in a second-order manner (Svirezhev et al., 1984). Fish uptake of X_{bh} (q_{XbhXf}) and X_{ba} (q_{XbaXf}) contribute to fish growth (q_{GXf}), together with pelleted feed ($q_{XfeedXf}$), which can be written as:

$$q_{GXf} = q_{XfeedXf}/FCR_{Xfeed} + q_{XbhXf}/FCR_{Xbh} + q_{XbaXf}/FCR_{Xba} \quad (6)$$

in which FCR_{Xfeed}, FCR_{Xbh}, and FCR_{Xba} are feed conversion ratios of X_{feed}, X_{bh}, and X_{ba}, respectively.

All components listed in Table A.2 leave the tank through water replacement, except for X_f, S_{co}, and S_o. Each of the tanks was considered to be ideally mixed. Hence, the concentration of components leaving the tank is similar to the concentration in the tank.

The model was implemented in Ms Excel and solved using the Euler forward method with a simulation time of 56 days and a time steps of one hour.

2.4. Sensitivity analysis, calibration, and validation

Sensitivity analysis (SA) was conducted by increasing and decreasing the parameters listed in Table A.4 by 50 %. Parameters with the highest normalized sensitivity coefficient (S_{yx}) (Tarigan et al., 2024) were prioritized in the calibration steps.

Calibration was done by fitting the corresponding model outputs to S_{nh}, S_{no}, S_{nd}, and biofloc data using a trial and error method. For the calibration the Control-diet dataset of Tarigan et al. (2025) was used. The fit is expressed in terms of as the ratio between the root mean square error (RMSE) to the average of observation data (μ) or RMSE/μ, aiming to find the lowest RMSE/μ. Further, RMSE/μ is called as normalised RMSE (NRMSE). In the experiment of Tarigan et al. (2025), biofloc was defined as solid residue after tank water was filtered using Whatman paper. In the simulation, biofloc is defined as a combination of X_s, X_p, X_{bh}, and X_{ba} because solids residue can contain alive (X_{bh} and X_{ba}) and dead (X_s and X_p) particulate organic matters. The calibrated model was cross-validated using the High-NSP-diet dataset of Tarigan et al. (2025) to understand the model performance under different diet compositions.

In the cross-validation step, deliberately the same parameter value as in the calibration step were used, except for some parameters related to fish and feed characteristics, which are apparent digestibility of organic matter by the fish body (ADC_{OM}), the FCR, the nitrogen retention efficiency of the fish body (REN_{Xf}), and the nitrogen content of the feed (N_{feed}) (Table 1).

3. Results

3.1. Sensitivity analysis and parameterization

Compared to other components mentioned in Section 2.2, X_{bh} and X_p are the most sensitive model outputs, represented by a higher S_{yx} (Fig. 2). The maximum S_{yx} of X_{bh} and X_p are around 11, while the maximum S_{yx} of other model outputs is around 0.1–1.64. In general, parameters with the highest S_{yx} are related to X_{bh}, such as the X_{bh} yield (Y_h), the maximum growth rate of X_{bh} (μ_h), the hydrolysis coefficient of X_{bh} (k_h), and the decay rate of X_{bh} (b_h). Parameters related to X_{ba} (Y_a, μ_a, and b_a) had a relatively have lower S_{yx} than X_{bh}, which means that changing parameters related to X_{ba} have a lower effect on the model output. However, these parameters were considered in the calibration step of S_{no} as Y_a and μ_a have the highest S_{yx} in S_{no}.

In terms of nitrogen balance, S_{nh} and S_{no} were mostly sensitive to fish-related parameters, which are the apparent digestibility of OM (ADC_{OM}) and the retention efficiency of nitrogen in fish biomass (REN_{Xf}).

Based on the sensitivity analysis, five parameters with the highest S_{yx} were prioritized to be adjusted in the calibration step, namely Y_h, b_h, μ_h, k_h, and α_g. Another three parameters related to X_{ba} were also adjusted, which were i_{xb}, b_a, and μ_a. Although these parameters have low S_{yx} (-0.1–0.8), they are essential in determining the dynamics of S_{nh} and S_{no}. Finally, another parameter, which is k_a, was chosen for the sake of S_{nd} fitting. S_{yx} values of all parameters to S_{nd} were close to zero, and therefore not shown in Fig. 2. Consequently, fitting S_{nd} might include calibration of more than one parameter or more than 50 % adjustment compared to the initial value. Based on the sensitivity analysis, adjustment of b_h, μ_h, and k_h can shift the dynamics of S_{nd}. However, it still resulted in NRMSE of S_{nd} and S_{no} of 74 % and 86 %, respectively. One of the highest S_{yx} values in S_{nd} (after b_h, μ_h, and k_h) was k_a ($S_{yx} = -0.021$) and was chosen to be adjusted. The calibrated value of all

Table 1
Diet-dependent parameter estimates value during calibration (Control-diet) and validation (High-NSP-diet) process.

Parameters	Control-diet	High-NSP-diet	Units
ADC_{OM}	0.60	0.48	-
FCR	1.42	1.64	g dry weight feed (g fresh weight fish)$^{-1}$
REN_{Xf}	32.1	31.2	%
N_{feed}	0.047584	0.043748	g N (g dry weight feed)$^{-1}$

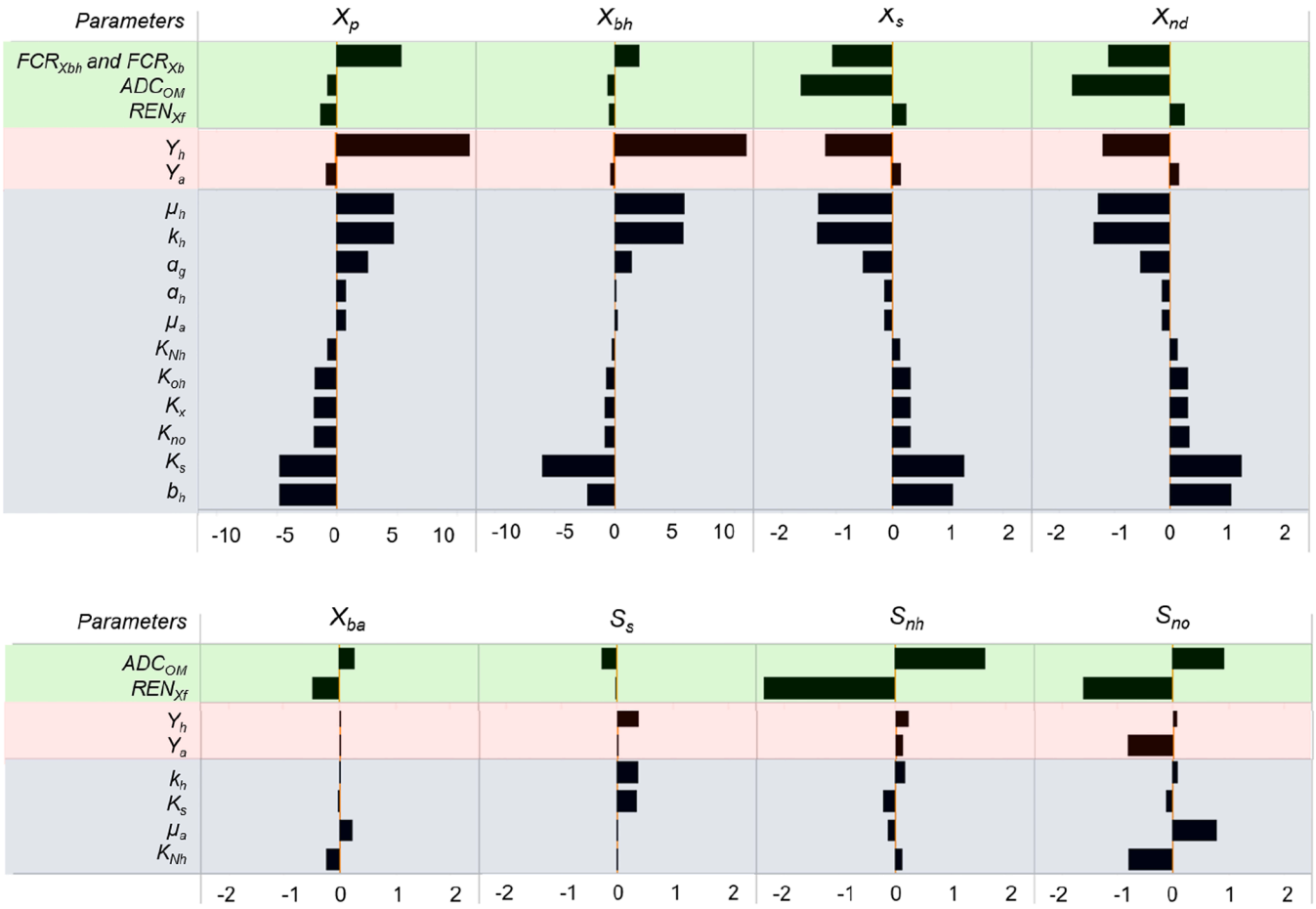

Fig. 2. Normalized sensitivity coefficients (S_{yx}) of different parameters to model output of X_{bh}, X_{ba}, X_p, X_s, X_{nd}, S_{nd}, S_s, S_{nh}, and S_{no}. Greenish, reddish, and bluish background colors indicate fish-related, stoichiometric, and kinetic parameters, respectively.

aforementioned parameters are shown in Table 2.

3.2. Model simulations

The parameters presented in Table 2 and Table A.4 were used to simulate components mentioned in Section 2.2. Model fitting was performed for X_f, S_{nh}, S_{no}, S_{nd}, and VSS, in which VSS is the summation of X_s, X_p, X_{bh}, and X_{ba}. Using the calibrated parameters (Table 2 and Table A.4), the simulation fitted the value of the final harvested fish (X_f) with a 3 %-5 % error (NRMSE) as shown in Table 3. In general, the simulation was able to depict the dynamics of S_{nh}, S_{no}, S_{nd}, and VSS of the Control-diet datasets with NRMSE of 0.15–0.34. However, simulation with the calibrated parameters in tanks fed with the High-NSP-diet resulted in relatively higher error. The highest error was observed in VSS with NRMSE of 0.66, followed by S_{nh} and S_{no} with NRMSE of 0.64 and 0.36, respectively (Table 3). Since VSS consists of X_{bh} and X_{ba}, which have a direct relationship to X_s, S_s, S_{nh}, and S_{no}, a high error of VSS also leads to a higher error in S_{nh} and S_{no}. Therefore, more detail observation of the dynamics of VSS of the High-NSP-diet datasets is required to understand the reasons for the higher error compared to the Control-diet datasets (see 3.3.2 and 4.2).

3.3. Nutrient and biofloc dynamics

3.3.1. Control-diet

Hourly simulations data and biweekly observations of S_{nh}, S_{no}, S_{nd}, and VSS in tanks fed the Control-diet tank are depicted in Fig. 3. The effect of daily feeding, especially in the fluctuation of Snh and VSS are clearly visible in Figs. 3a and 3d, respectively. A relatively stable behaviour of S_{nh} and increasing behaviour of S_{no} (Fig. 3a and Fig. 3b) is observed, indicating an active conversion of S_{nh} into S_{no}. S_{nh} was constantly added into the water via S_{nd} ammonification and fish digestion(Fig. 1). Accumulation of S_{nh} in the water was controlled by X_{bh} uptake and X_{ba} conversion during nitrification, causing S_{no} accumulation (Fig. 1). In terms of S_{nd}, the decreasing trend (Fig. 3c) was mainly due to water replacement and less due to ammonification. Since the tanks are assumed to be ideally mixed, a higher initial S_{nd} concentration (39 g/m^3) means the loss of S_{nd} through water exchange when compared to the initial mass of S_{nh} and S_{no} (0.4 g/m^3). Finally, the behaviour of VSS in the simulation aligned with the observation, increasing from day 0 to day 42 and decreasing slightly from day 42 to day 56 (Fig. 3d).

In the VSS, biofloc biomass was dominated by X_s and X_{bh} (Fig. 4a) and relatively a small amount of X_p and X_{ba} (Fig. 4b). The drop of VSS from day 42 to day 56 (Fig. 3d) was mainly caused by the drop of X_s (Fig. 4a). This drop was primarily driven by the drastic increase in X_{bh} during this period. X_{bh} plays a role in hydrolysing X_s into S_s in which the rate is linear to X_{bh} (Equation A.14). In other words, an increase of X_{bh} will eventually lower X_s accumulation in the water when the input of X_s is lower than the X_s hydrolysed into S_s. Regarding X_{ba}, the biomass concentration was relatively stable with 0.6–1 g COD/m^3 (Fig. 4b). Such amount of X_{ba} contributes to 23 % of the S_{nh} level with a maximum of 0.67 g/m^3 (Fig. 3a). Almost 75 % of the S_{nh} reduction was caused by X_{bh} uptake. Although the majority of S_{nh} reduction was caused by X_{bh} uptake, a change of 1 g of X_{ba} was 182 times higher than a change of 1 g of X_{bh} in reducing S_{nh} concentration in the water. Based on Table A.2 (Equation A.26 and A.27), 1 g of X_{ba} growth consumed 4.19 g of S_{nh}, while 1 g of X_{bh} only consumed 0.023 g of S_{nh}.

The increase of X_{bh} will increase and decrease S_{nd} simultaneously

Table 2
Initial and final parameters estimates during the calibration process. Initial value was gained from ASM number 1 (Henze et al., 1987), which are parameters of domestic wastewater.

Parameters	Description	Units	Initial value	Calibrated value
Y_h	Yield for heterotrophic biomass	g cell COD formed (g COD oxidized)$^{-1}$	0.67	0.75
b_h	Decay coefficient for heterotrophic biomass	h^{-1}	0.0258	0.0019
μ_h	Maximum specific growth rate for heterotrophic biomass	h^{-1}	0.25	0.0375
k_h	Maximum specific hydrolysis rate	g slowly biodegradable COD (g cell COD. h)$^{-1}$	0.125	0.0238
α_g	Correction factor for μ_h under anoxic conditions	-	0.8	2
i_{xb}	Nitogen required per for the growth of X_{bh} and X_{ba}	g N (g COD)$^{-1}$ in biomass	0.086	0.0234
b_a	Decay coefficient for autotrophic biomass	h^{-1}	-	0.00014
μ_a	Maximum specific growth rate for autotrophic biomass	h^{-1}	0.033	0.0027
k_a	1/Ammonification rate	m^3 (g COD. h)$^{-1}$	0.0033	0.00002

Table 3
Normalized root mean square error (NRMSE) of the Control-diet and the High-NSP-diet dataset. NRMSE is the ratio of RMSE to average observation value (RMSE/μ).

		X_f	S_{nh}	S_{no}	S_{nd}	VSS
Control-diet	RMSE	361.9	0.66	2.53	69.44	114.07
	NRMSE	6 %	20 %	29 %	34 %	15 %
High-NSP-diet	RMSE	225.5	2.30	3.55	55.70	600.64
	NRMSE	4 %	64 %	36 %	23 %	66 %

through hydrolysis (conversion from X_{nd} into S_{nd}, see Equation A.14 and A.22) and ammonification (conversion from S_{nd} into S_{nh}, see Equation A.23), respectively. A higher kinetics parameter of hydrolysis than of ammonification caused a slight increase of S_{nd}. The increase of S_{nd} becomes more significant when X_{bh} increased more strongly from day 42 to day 56 (Fig. 3c and Fig. 4a).

3.3.2. High-NSP-diet

The highest NRMSE (66 %) in the High-NSP-diet is observed for VSS (Table 2). The discrepancy is particularly found on day 42 (Fig. 5a) in which total biofloc biomass was much higher than the predicted biomass (204 vs 302 g COD/m^3). This discrepancy is most likely caused by X_s or X_{ba} which are the dominant components in the VSS (Fig. 5b). From day 37–42, X_s dropped from around 114 g COD/m^3 to around 10 g COD/m^3. This drastic drop was triggered by the increase in hydrolysis rate (conversion from X_s to S_s), which was encouraged by the rise of X_{bh} over time from day 37 to day 42. A relatively high discrepancy is also observed in S_{nh} and S_{no} with NRMSE of 64 % and 36 % (Table 2), respectively, in which most of the error is caused by under-prediction and a sudden over-prediction of S_{nh} on day 56 (Fig. 5c and Fig. 5d). Based on the simulation, some parameters related to X_{bh} and X_{ba} might need to be adjusted further to achieve a better fit in Hight-NSP-diet fed biofloc tanks, and will be discussed in Section 4.

4. Discussion

4.1. Feedback loop

This study presents the dynamic behaviour of biofloc in Nile tilapia culture. Interactions between different components in the fish-biofloc systems can be depicted in a causal loop diagram (Fig. 6). Two reinforcing feedback loops and nine balancing feedback (Barbrook-Johnson and Penn, 2022) loops were identified. More feedback loops might have occurred. These are not shown in this graph, for instance, a feedback loop between fish growth and fish mortality to fish biomass.

There is a balancing feedback loop interaction between X_{bh} and X_s as depicted in Fig. 6. Uneaten feed, fish faeces, and decay of micro-organisms were introduced to the activated sludge system in the form of X_s, which will subsequently be hydrolysed into S_s. In turn, S_s is incorporated into X_{bh}, causing an increase in X_{bh} biomass. In other words, an increase of X_s leads to an increase of S_s and possibly X_{bh}. However, there are both a reinforcing and balancing feedback loop between X_{bh} and X_s. The reinforcing loop is triggered by the fact that more biomass will decay as more X_{bh} becomes available in the water (R1 in Fig. 6), which is one of the inputs to X_s. However, as more X_{bh} is available in the water, it will increase the hydrolysis process, causing a faster drop of X_s (B.1 in Fig. 6). In this study, the biomass decay rate was almost 10 times lower as compared to hydrolysis process rate, both in the Control-diet and High-NSP-diet tanks. Additionally, a balance occurred between the X_{bh} and S_s feedback loop. The increasing concentration of X_{bh} means more S_s is required for X_{bh} growth, which eventually will decrease S_s when the uptake rate is higher than the hydrolysis rate (q_{SsXbh} (Equation A.15) and q_{XsSs} (Equation A.14), respectively).

The balancing feedback loop in tanks fed the Control-diet was observed after day 42 when X_s started to decrease (Fig. 4a). The growth rate of X_{bh} overall increased until day 53. Since the simulation was only carried out until the end of the experiment on day 56, the decreasing growth rate was hardly seen (Fig. 4a). The late drop of X_{bh} growth rate was triggered by S_s that was still available before finally dropping on day 53 due to a limited supply through hydrolysis of X_s (see Fig. 5b and Figure B.1).

A similar feedback loop is also observed between X_{bh} and nitrogen components (X_{nd}, S_{nd}, and S_{nh}). A reinforcing feedback loop occurs due to X_{bh} decay (R2 in Fig. 6). Two balancing feedback loops occur, one between X_{bh} growth and S_{nh} uptake (B5 in Fig. 6), another one between X_{bh} and X_{nd} due to hydrolysis of X_{nd} into S_{nd} and ammonification of S_{nd} into S_{nh} (B3 in Fig. 6). Additionally, S_{nh} is not only balanced by X_{bh} uptake but also by X_{ba} uptake (B6 in Fig. 6). Finally, the relationship between fish and X_{bh} and X_{ba} is also expressed in a balancing feedback loop. A higher X_{bh} and X_{ba} lead to higher uptake by fish which will boost the fish growth. However, a higher consumption of X_{bh} and X_{ba} will reduce these micro-organism concentrations. In summary, several balancing feedbacks are observed in the fish-biofloc system. Understanding the balance will give insight on maintaining the continuity of the fed-batch fish-biofloc system.

4.2. Improving simulation of the High-NSP-diet

The fish-ASM shows a relatively high discrepancy of VSS, S_{nh}, and S_{no} in tanks fed the High-NSP-diet (Table 3). The error in VSS is mostly caused by X_s or X_{bh}, which are the dominant components in VSS (Fig. 5b). The error might be related to a temporal change in some of the parameter values, especially parameters related to the micro-organisms (X_{ba} and X_{bh}). The High-NSP-diet dataset was used for cross-validation of the fish-ASM, which means using the same, except those mentioned in Table 1, parameter values as in the Control-diet simulation. A diet rich in NSP produces more fiber-rich faeces, which require more time to decompose as compared to starch-rich faeces (Avnimelech et al., 2009; Ekasari et al., 2014; Serra et al., 2015). This difference in the faeces

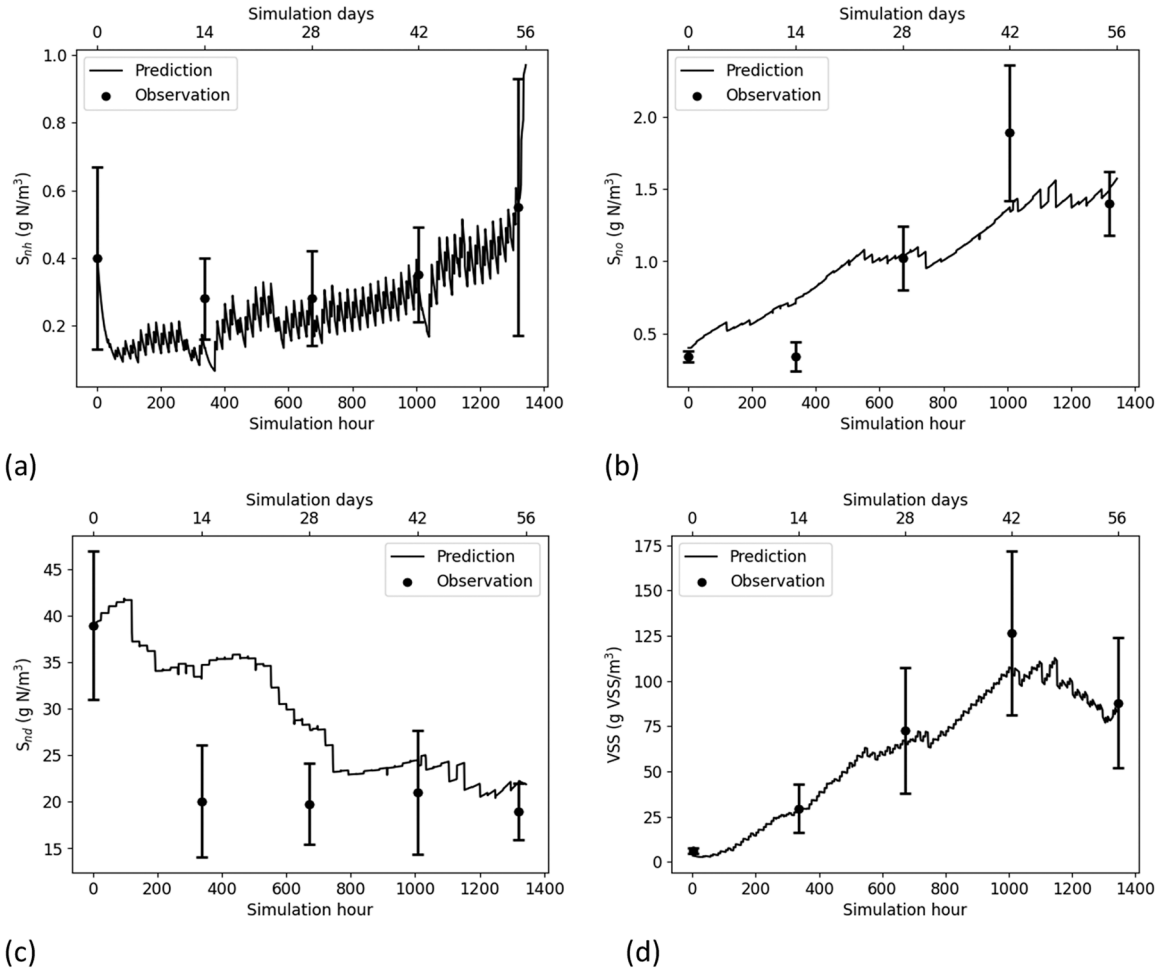

Fig. 3. Model predictions and observation data of (a) ammonia nitrogen (S_{nh}), (b) nitrate + nitrite nitrogen (S_{no}), (c) soluble organic nitrogen (S_{nd}), and (d) volatile suspended solide (VSS) or biofloc in the Control-diet case.

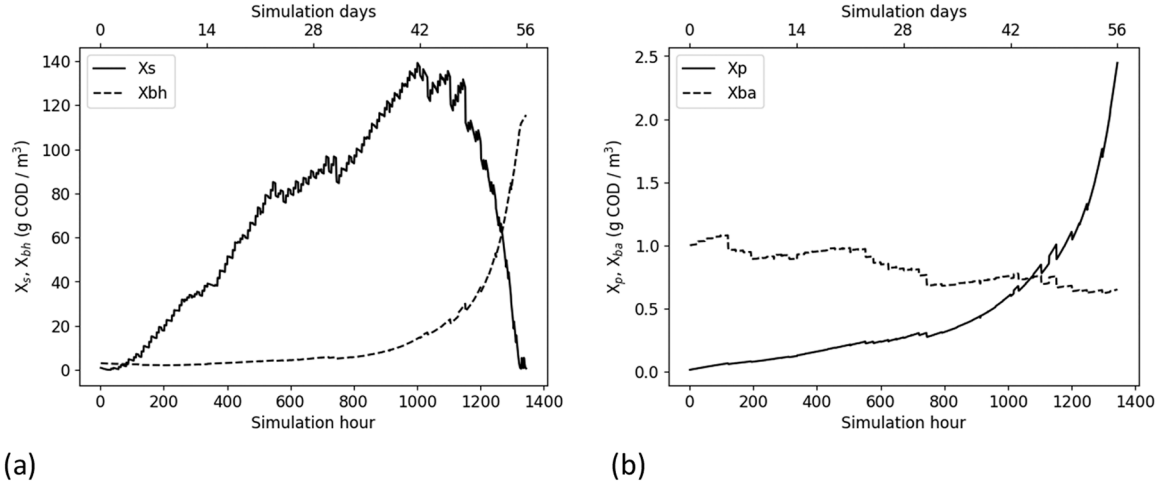

Fig. 4. Hourly simulation data of VSS based on its constituent components, which are (a) Xs, Xbh, and (b) Xp, and Xba, in Control-diet case in g COD/tank.

might cause a difference in hydrolysation rate between the between tanks fed the Control-diet or the High-NSP-diet. Slower hydrolysis in tanks fed the High-NSP-diet was not integrated in the model, and therefore not studied.

Improving the simulation-observation fit of the High-NSP-diet tanks by adjusting some parameters could be done based on the highest sensitivity coefficient S_{yx} (Fig. 2). Additionally, the most interesting parameters might be related to X_{bh} and X_{ba} which have a direct relationship to VSS and S_{nh} which exhibited the highest NRMSE in tanks fed the High-NSP-diet. Changing the $Y_{h,}$ parameters with the highest S_{yx} relative to X_{bh} (Fig. 2), from 0.75 to 0.71 improves the NRMSE of VSS from 66 % to 47 % (Table 3 and Table B.1). A lower Y_h means that less g

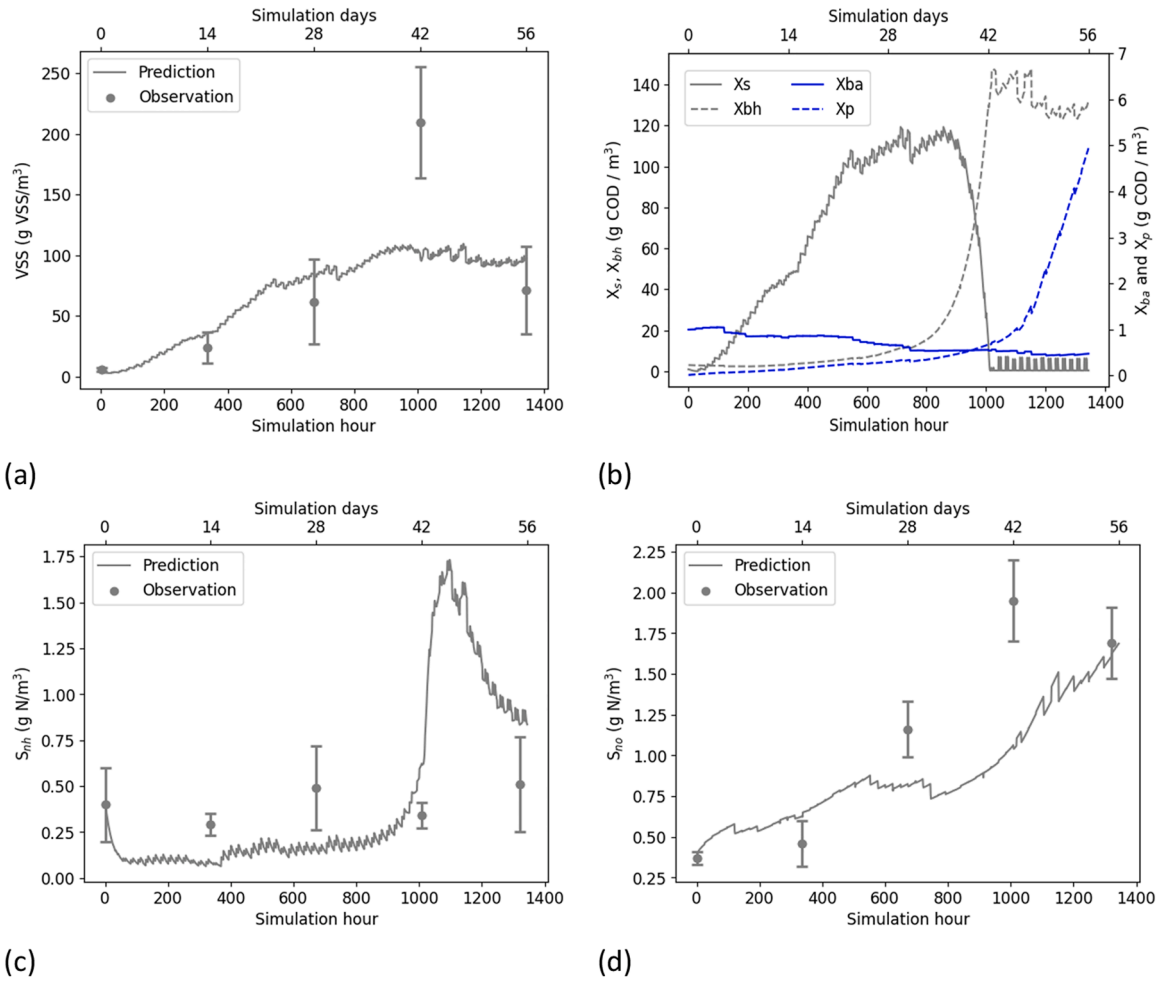

Fig. 5. Model predictions and observation data of(a) volatile suspended solid (VSS), (b) partial components of VSS: X_s, X_{bh}, X_p, and X_{ba}, (c) ammonia nitrogen (S_{nh}), and (d) nitrate + nitrite nitrogen (S_{no}) in the High-NSP-diet case.

cell COD X_{bh} formed per g S_s uptake by X_{bh}. Less X_{bh} production means more X_s will be accumulated due to the lower hydrolysis rate. Compared to the value of Y_h of 0.75, the updated value of 0.71 increases the VSS on day 42, which is caused by more X_s accumulating (102 g VSS/m^3 vs 140 g VSS/m^3) in the system. After day 42, X_{bh} started to grow drastically, leading to faster hydrolysis, and eventually reduced X_s accumulation (Figure B.2a and Figure B.2b). The change of Y_h also affects the dynamics of S_{nh}, and eventually S_{no} (Figure B.2c and Figure B.2d), in which more S_{nh} will be accumulated at the end of the simulation due to higher ammonification of S_{nd} into S_{nh} by X_{bh} from day 42 to day 56. Hence, after adjusting Y_h, parameters related to S_{nh} also need to be adjusted to improve the fit between simulation and observation, such as Y_a (g cell COD of X_{ba} formed per g N uptaken by X_{ba}), i_{xb} (g N required per g COD biomass of X_{bh} and X_{ba}), and $1/k_a$ (g COD hydrolysed per h per m^3). Adjusted parameters, NRMSE, and new simulation results of S_{no} and S_{nh} are depicted in Table B.1, Table B.2, Figure B.2e, and Figure B.2 f, respectively.

Changing the aforementioned parameters can reduce the NRMSE of VSS and S_{nh}, however, the error was still around 50 % (Table B.1). In terms of VSS, this updated strategy can improve X_s concentration on day 42, but not the X_{bh} concentration. The hydrolysis process of X_s might be slower due to its high fiber content as compared to the Control-diet. Consequently, S_s production, one of the limiting factors of X_{bh} growth, is also lower compared to the Control-diet. However, since the High-NSP-diet has lower ADC_{OM} (Table 1), which means higher faeces production, the S_s production will eventually be higher than in tanks fed the Control-diet, which means a higher growth of X_{bh}. In this case, the higher VSS on day 42 in the High-NSP-diet when compared to the Control-diet (127 g VSS/m^3 vs 210 g VSS/m^3) was probably caused by a higher accumulation of X_s and a higher X_{bh} concentration in the water. Further research might be needed to understand the mechanisms and dynamics of the hydrolysis process and its relationship to X_{bh} in biofloc systems fed a High-NSP or fiber-rich diet.

5. Conclusion

To our knowledge, this is the first study that demonstrates the dynamics of nitrogen and biofloc in fish-biofloc systems. This study demonstrated the possibility of combining the ASM concept and nutrient-based fish growth modelling to understand the relationship between fish, organic matter, nitrogen, heterotrophic biomass, and autotrophic biomass in a fish-biofloc system. Simulation under Control-diet was considerably fit (NRMSE of around 15 %-34 %) to the field observation. However, improvement is needed in the simulation of the tank fed with the High-NSP-diet, especially in the biofloc and ammonia dynamics.

The High-NSP-diet datasets were simulated using a cross-validation technique, which means the simulation was performed based on calibrated parameters of Control-diet data. The inclusion of NSP was aimed to change fish faeces characteristics, which eventually will affect the hydrolysis rate and biofloc growth in the water. Further research might be focused on studying the mechanisms and dynamics of the hydrolysis of organic matter and its relationship to heterotrophic biomass in biofloc systems fed a high-NSP or fiber-rich diet.

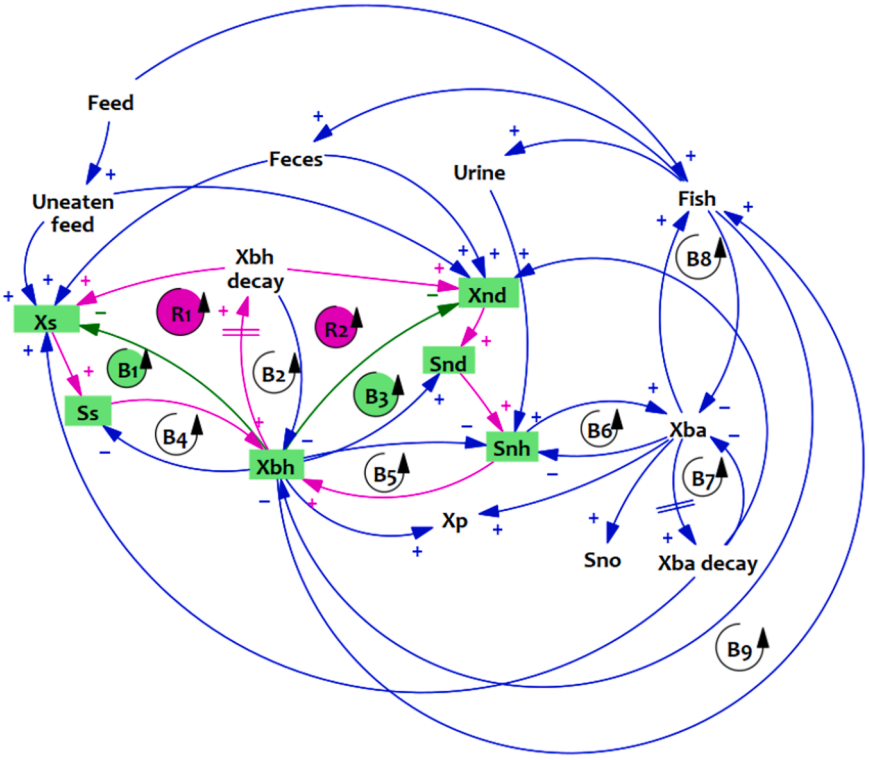

Fig. 6. Causal loop diagram of the fish-ASM.Bi = Balancing feedback loop i, Ri = Reinforcing feedback loop i, Xs = Particulate organic matter, S_s = Soluble organic matter, X_{bh} = Heterotrophic biomass, X_{nd} = Particulate organic nitrogen, S_{nd} = Soluble organic nitrogen, S_{nh} = Ammonia nitrogen, X_{ba} = Autotrophic biomass, X_p = Non-degradable organic matter. Pink arrows represent reinforcing feedback pathways of R1 and R2. Green arrows and colour represent balancing feedback pathways of B1 and B3.

Funding

This work was supported by Interdisciplinary Research and Education Fund (INREF), Wageningen University & Research

CRediT authorship contribution statement

Karel J Keesman: Writing – original draft, Validation, Supervision, Resources, Methodology, Funding acquisition, Data curation, Conceptualization. **Julie Ekasari:** Writing – review & editing. **Marc Verdegem:** Writing – review & editing, Validation, Supervision, Conceptualization. **Nurhayati Br Tarigan:** Writing – review & editing, Writing – original draft, Visualization, Software, Resources, Project administration, Methodology, Investigation, Formal analysis, Data curation, Conceptualization.

Declaration of Competing Interest

The authors declare that they have no known competing financial interests or personal relationships that could have appeared to influence the work reported in this paper.

Appendix A. Parameters and equations

Table A.1
Initial values used in the calibration (Control-diet) and validation (High-NSP-diet) process

Parameter	Value	Units
S_s	38.00	g COD m^{-3}
X_s	9.00	g COD m^{-3}
X_i	17.00	g COD m^{-3}
S_i	36.00	g COD m^{-3}
X_{bh}	3	g COD m^{-3}
X_{ba}	1	g COD m^{-3}
X_p	0.015	g COD m^{-3}
S_o	6	g COD m^{-3}
S_{no}	0.4	g N m^{-3}
S_{nh}	0.4	g N m^{-3}
S_{nd}	39	g N m^{-3}
X_{nd}	0.5	g N m^{-3}
S_{alk}	5	Molar

Table A.2
Mass balance equation of each compartment in the model

Compartment	Equation
Fish	$\frac{dX_f}{dt} = q_{GXf} - q_{MXf}$
Feed	$\frac{dX_{feed}}{dt} = U(t) - q_{XfeedXf} - q_{XfeedXs}$
Heterotrophic biomass	$\frac{dX_{bh}}{dt} = q_{GXbh} - q_{XbhXs} - q_{XbhXf} - q_{Xbhout}$
Autotrophic biomass	$\frac{dX_{ba}}{dt} = q_{GXba} - q_{XbaXs} - q_{XbaXf} - q_{Xbaout}$
Organic matter	$\frac{dX_s}{dt} = q_{XfXs} + q_{XfeedXs} + q_{XbhXs} + q_{XbaXs} - q_{XsSs} - q_{Xsout}$
	$\frac{dS_s}{dt} = q_{XsSs} - q_{SsXbh} - q_{Ssout}$
	$\frac{dX_p}{dt} = q_{XbhXp} + q_{XbaXp} - q_{Xpout}$
Nitrogen	$\frac{dX_{nd}}{dt} = q_{XfXnd} + q_{XfeedXnd} + q_{XbhXnd} + q_{XbaXnd} - q_{XndSnd} - q_{Xndout}$
	$\frac{dS_{nd}}{dt} = q_{XndSnd} - q_{SndSnh} - q_{Sndout}$
	$\frac{dS_{nh}}{dt} = q_{XfSnh} + q_{SndSnh} - q_{SnhXbh} - q_{SnhXba} - q_{Snhvolat} - q_{Snhout}$
	$\frac{dS_{no}}{dt} = q_{XbaSno} - q_{SnoXbh} - q_{Snoout}$
Oxygen	$\frac{dSo}{dt} = q_{Sopump} + q_{Sosurface} - q_{XfSo} - q_{XbhSo} - q_{XbaSo} - q_{Soout}$
Carbon dioxide	$\frac{dSco}{dt} = q_{ScoXf} + q_{ScoXbh} + q_{ScoXba} - q_{Scoout}$
Alkalinity	$\frac{dSalk}{dt} = q_{SndSalk} - q_{SalkXbh} - q_{SalkXba}$

Table A.3
Auxiliary equations of each flow in the mass balance

	Process name	Equations	Eqn
Fish and Feed			
q_{GXf}	Fish growth	$q_{XfeedXf}/FCR_{Xfeed} + q_{XbhXf}/FCR_{Xbh} + q_{XbaXf}/FCR_{Xba}$	A.1
q_{MXf}	Fish mortality	$X_f * km$	A.2
$q_{XfeedXf}$	Feed uptaken by fish	$U(t) * (1-ku)$	A.3
$q_{XfeedXs}$	Feed uneaten	$U(t) * ku$	A.4
Heterotrophic biomass			
$q_{GXbh, aerobic}$	Aerobic growth of heterotrophs	$\mu_h * (S_s/(S_s+K_s)) * (S_o/(S_o+K_{oh})) * X_{bh}$	A.5
$q_{GXbh,anoxic}$	Anoxic growth of heterotrophs	$q_{GXbh,aerobic} * (S_{no}/(S_{no}+K_{no})) * \alpha_g$	A.6
q_{GXbh}	Total growth of heterotrophs	$q_{GXbh,aerobic} + q_{GXbh,anoxic}$	A.7
q_{XbhXs}	Decay of heterotrophs	$b_h * X_{bh}$	A.8
q_{XbhXf}	Heterotrophs uptaken by fish	$X_f * \mu_{XbhXf} * (X_{bh}/(K_{XbhXf}+X_{bh}))$	A.9
Autotrophic biomass			
q_{GXba}	Growth of autotrophs	$\mu_a * (S_{nh}/(S_{nh}+K_{nh})) * (S_o/(S_o+K_{oa})) * X_{ba}$	A.10
q_{XbhXs}	Decay of autotrophs	$b_a * X_{ba}$	A.11
q_{XbaXf}	Autotrophs uptaken by fish	$X_f * \mu_{XbaXf} * (X_{ba}/(K_{XbaXf}+X_{ba}))$	A.12
Organic matter			
q_{XfXs}	Fish faeces production	$(1 - ADC_{OM}) * (q_{XfeedXf} + q_{XbhXf} + q_{XbaXf})$	A.13
q_{XsSs}	Hydrolysis of entrapped organics	$k_h * [(X_s/X_{bh})/((X_s/X_{bh}) + K_x)] * [(S_o/(S_o+K_{oh})) + \alpha h * (K_{oh}/(S_o+K_{oh})) * (S_{no}/(S_{no}+K_{no}))] * X_{bh}$	A.14
q_{SsXbh}	Readily biodegradable substrate uptaken by heterotrophic biomass	$1/Y_h * q_{GXbh}$	A.15
q_{XbhXp}	Heterotrophic biomass become non-degradable particulate organic	$f_p * q_{XbhXs}$	A.16
q_{XbaXp}	Autotrophic biomass become non-degradable particulate organic	$f_p * q_{XbaXs}$	A.17
Nitrogen			
q_{XfXnd}	Particulate organic nitrogen from fish faeces	$(1 - ADC_{OM}) * (N_{Xfeed} * q_{XfeedXf} + N_{Xbh} * q_{XbhXf} + N_{Xba} * q_{XbaXf})$	A.18
$q_{XfeedXnd}$	Particulate organic nitrogen from uneaten feed	$N_{Xfeed} * q_{XfeedXs}$	A.19
q_{XbhXnd}	Particulate organic nitrogen from heterotrophics biomass decay	$(i_{xb} - f_p*i_{xp}) * q_{XbhXs}$	A.20
q_{XbaXnd}	Particulate organic nitrogen from autotrophics biomass decay	$(i_{xb} - f_p*i_{xp}) * q_{XbaXs}$	A.21
q_{XndSnd}	Hydrolysis of entrapped organic N	$q_{XsSs} * X_{nd}/X_s$	A.22
q_{SndSnh}	Ammonification of soluble organic N	$ka * S_{nd} * X_{bh}$	A.23
q_{XfSnh}	Fish total ammonia nitrogen (TAN) production	$q_{XNXf} - REN_{Xf}*q_{XNXf} - q_{XfXnd}$	A.24
q_{XNXf}	Nitrogen from feed, heterotrophics, and autotrophics biomass taken up by fish	$N_{Xfeed}*q_{XfeedXf} + N_{Xbh}*q_{XbhXf} + N_{Xba}*q_{XbaXf}$	A.25
q_{SnhXbh}	TAN uptake by heterotrophics biomass	$i_{xb} * q_{GXbh}$	A.26
q_{SnhXba}	TAN uptake by autotrophics biomass	$(i_{xb} + 1/Y_a)* q_{GXba}$	A.27
$q_{Snhvolat}$	TAN volatilization	$kv * S_{nh}$	A.28
q_{XbaSno}	Nitrification by autotrophics biomass	$1/Y_a * q_{GXba}$	A.29

(*continued on next page*)

Table A.3 (*continued*)

	Process name	Equations	Eqn
q_{SnoXbh}	Nitrate and nitrite nitrogen uptake by heterotrophics biomass in anoxic condition	$(1\text{-}Y_h)/(2.86 * Y_h) * q_{GXbh,anoxic}$	A.30
Oxygen			
q_{XfSo}	Oxygen uptake by fish	$2014.45 + 2.75 * X_f - 165.2 * T_w + 0.007 * X_f^2 + 3.93 * T_w^2 - 0.21 * X_f * T_w^4$	A.31
q_{XbhSo}	Oxygen uptake by heterotrophics biomass	$(1\text{-}Y_h)/Y_h * q_{GXbh}$	A.32
q_{XbaSo}	Oxygen uptake by autotrophics biomass	$(4.57\text{-}Y_a)/Y_a * q_{GXba}$	A.33
Carbon dioxide			
q_{ScoXf}	Fish CO_2 respiration	$kcoX_f * X_f$	A.34
q_{ScoXbh}	CO_2 emission due to decay of heterotrophics biomass	$kcoX_{bh} * q_{XbhXs}$	A.35
q_{ScoXba}	CO_2 emission due to decay of autotrophics biomass	$kcoX_{ba} * q_{XbaXs}$	A.36
Alkalinity			
$q_{SndSalk}$	Alkalinity production due to ammonification of soluble organic N	$1/14 * q_{SndSnh}$	A.37
$q_{SalkXbh}$	Alkalinity consumption due to growth of heterotrophics biomass	$(i_{xb}/14) * q_{GXbh,aerobic} + (i_{xb}/14 - (1\text{-}Y_h)/14 * 2.86Y_h) * q_{GXbh,anoxic}$	A.38
$q_{SalkXba}$	Alkalinity consumption due to growth of autotrophics biomass	$(i_{xb}/14 + 1/7Y_a) * q_{GXba}$	A.39

Table A.4
Parameter value used for the simulation

Parameter	Description	Value	Unit	Reference
FCR_{Xfeed}	Feed conversion ratio of pelleted feed	1.42	g dry weight g^{-1} fresh weight	Tarigan et al., (2025)
FCR_{Xbh}	Feed conversion ratio of X_{bh}	2	g dry weight g^{-1} fresh weight	Stanley and Jones, (1976)
FCR_{Xba}	Feed conversion ratio of X_{ba}	2	g dry weight g^{-1} fresh weight	Stanley and Jones, (1976)
km	Coefficient of mortality			See Figure C.2 of Tarigan et al., (2024)
ku	Uneaten feed	5 %	-	Assumed
μ_h	Maximum growth rate of X_{bh}	0.0375	h^{-1}	Calibrated
K_s	Half saturation coefficient of S_s	20	g COD m^{-3}	Henze et al., (1987)
K_{oh}	Half saturation coefficient of S_o for the growth of X_{bh}	0.2	g O_2 m^{-3}	Henze et al., (1987)
K_{no}	Half saturation coefficient of S_{no}	0.5	g NO_3-N m^{-3}	Henze et al., (1987)
α_g	Correction factor for X_{bh} growth in anoxic condition	2	-	Calibrated
b_h	Decay rate of X_{bh}	0.0019	h^{-1}	Calibrated
μ_{XbhXf}	Maximum uptake rate of X_{bh} by fish (X_f)	0.00042	h^{-1}	Calibrated
K_{XbhXf}	Half saturation coefficient of X_{bh}	20	g COD m^{-3}	Svirezhev et al., (1984)
μ_a	Maximum growth rate of X_{ba}	0.003	h^{-1}	Calibrated
K_{nh}	Half saturation coefficient of S_{nh}	1	g NH_3-N m^{-3}	Henze et al., (1987)
K_{oa}	Half saturation coefficient of S_o for the growth of X_{ba}	0.4	g O_2 m^{-3}	Henze et al., (1987)
b_a	Decay rate of X_{bh}	0.00014	h^{-1}	Calibrated
μ_{XbaXf}	Maximum uptake rate of X_{bh} by fish (X_f)	0.00042	h^{-1}	Calibrated
K_{XbaXf}	Half saturation coefficient of X_{bh}	20	g COD m^{-3}	Svirezhev et al., (1984)
ADC_{OM}	Apparent digestibility coefficient of organic matter	0.6	-	Tarigan et al., (2025)
k_h	Hydrolysis rate	0.0238	g slowly biodegradable COD (g cell COD. $h)^{-1}$	Calibrated
K_x	Half saturation coefficient of hydrolysis of X_s by X_{bh}	0.03	g slowly biodegradable COD (g cell COD)$^{-1}$	Henze et al., (1987)
Y_h	X_{bh} yield	0.75	g cell COD formed (g COD oxidized)$^{-1}$	Calibrated
f_p	Ratio of X_{bh} and X_{ba} decay become non-degradable particulate (X_p)	0.08	-	Henze et al., (1987)
N_{Xfeed}	Nitrogen content of feed	0.047584	g N (g feed)$^{-1}$	Tarigan et al., (2025)
N_{Xbh}	Nitrogen content of X_{bh}	0.0599	g N (g X_{bh} COD)$^{-1}$	Tarigan et al., (2025)
N_{Xba}	Nitrogen content of X_{ba}	0.0599	g N (g X_{bh} COD)$^{-1}$	Tarigan et al., (2025)
i_{xb}	Nitrogen requirement per g COD biomass synthesised	0.0234	g N (g COD)$^{-1}$ in biomass	Calibrated
i_{xp}	Nitrogen requirement per g COD endogenous biomass synthesised	0.06	g N (g COD)$^{-1}$ in endogenous biomass	Henze et al., (1987)
k_a	Ammonification rate	0.00001	m^3 (g COD. $h)^{-1}$	Calibrated
REN_{Xf}	Nitrogen retention efficiency in fish body	0.321	-	Tarigan et al., (2025)
kv	Volatilization coefficient	0.00319	h^{-1}	Wolfe et al., (1986)
Y_a	X_{ba} yield	0.24	g cell COD formed (g N oxidized)$^{-1}$	Henze et al., (1987)
T_w	Water temperature		℃	See Figure C.1 of Tarigan et al., (2024)
$kcoX_f$	CO_2 emission	0.00026	g CO_2 (g fish. $h)^{-1}$	Muller and Bauer, (1994)
$kcoX_{bh}$	CO_2 emission of X_{bh} decay	2	g CO_2 (g biomass decay)$^{-1}$	Snip, (2010)
$kcoX_{ba}$	CO_2 emission of X_{bh} decay	2	g CO_2 (g biomass decay)$^{-1}$	Snip, (2010)

Appendix B. Simulation results

Table B.1
Root mean square error (RMSE) and normalise RMSE (NRMSE), which is ratio of RMSE to average observation value, of High-NSP-diet dataset after updating the parameters (see Table B2)

	X_f	S_{nh}	S_{no}	S_{nd}	VSS
RMSE	361.1	2.04	2.69	57.02	430.44
NRMSE	6 %	57 %	27 %	23 %	47 %

Table B.2
Adjusted parameters in the High-NSP-diet tank

Parameters	Initial value	Adjusted value	Units
Y_h	0.75	0.71	g cell COD formed (g COD oxidized)$^{-1}$
Y_a	0.24	0.1	g cell COD formed (g N oxidized)$^{-1}$
i_{xb}	0.003	0.004	g N (g COD)−1 in biomass
k_a	0.00002	0.000003	m^3 (g COD. h)$^{-1}$

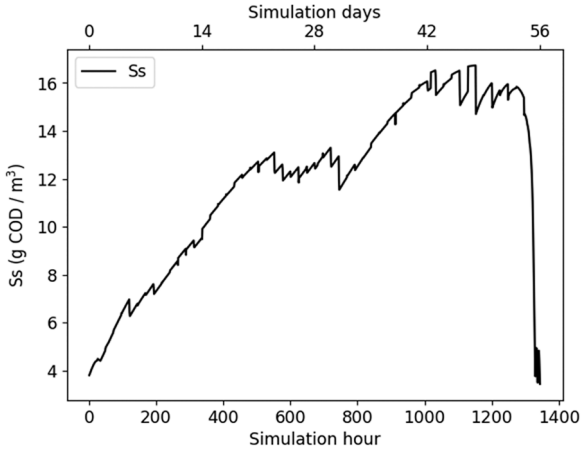

Fig. B.1. Simulation result of S_s in the Control-diet tank

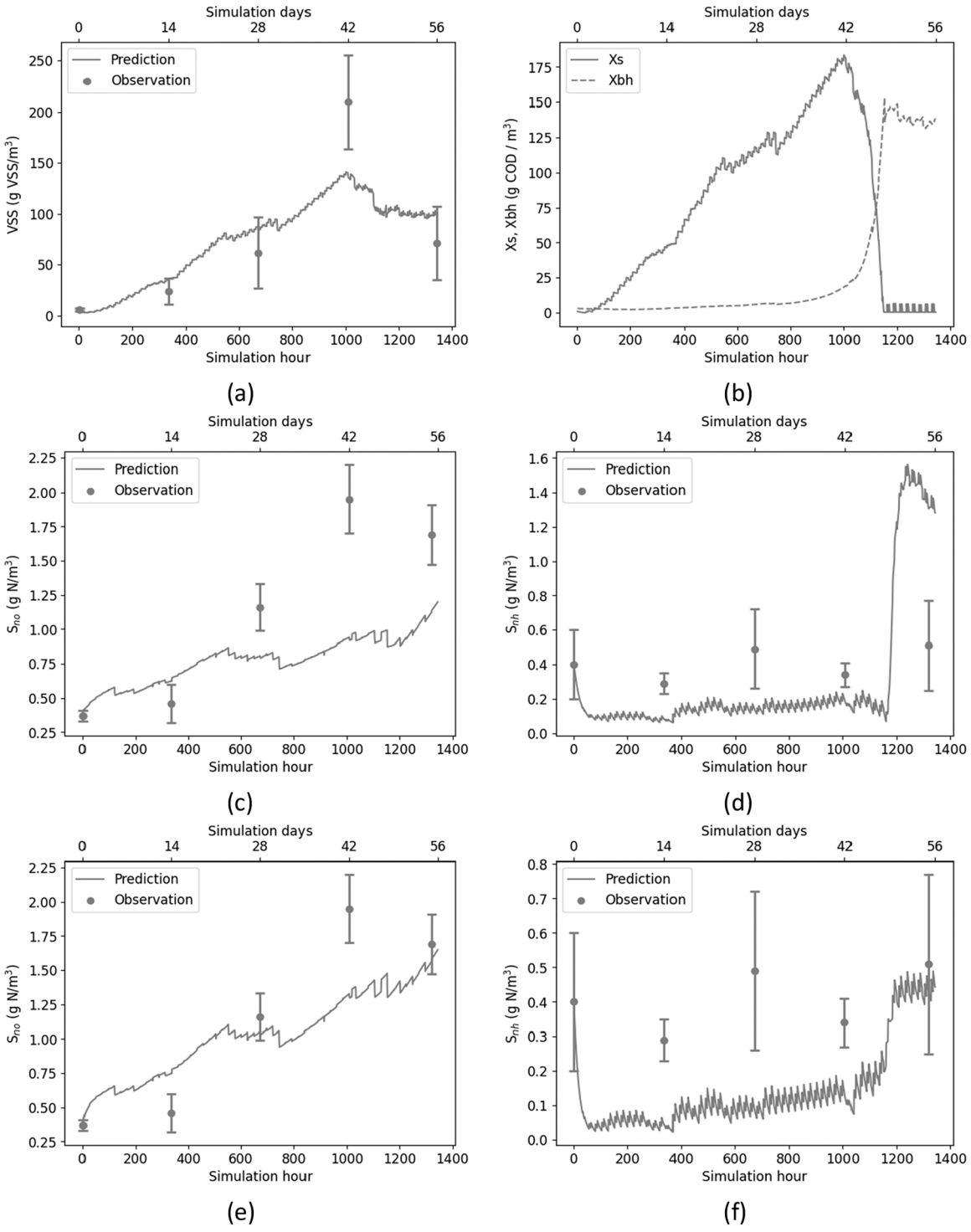

Fig. B.2. Updated model prediction and observation data when $Y_h = 0.71$ (a. volatile suspended solid (VSS) or biofloc, b. detail component of VSS, c. nitrate + nitrite nitrogen (S_{no}), d. ammonia nitrogen when Y_h is 0.71), and when all parameters is adjusted as shown in Table B.2 (e. S_{no}, f. S_{nh}) of the High-NSP-diet datasets

Data availability

Data will be made available on request.

References

Avnimelech, Y., 2009. Biofloc technology: a practical guide book. World Aquaculture Society.

Barbrook-Johnson, P., Penn, A.S., 2022. Causal loop diagrams. In *Systems Mapping: How to build and use causal models of systems*. Springer International Publishing, Cham, pp. 47–59. https://doi.org/10.1007/978-3-031-01919-7_4.

Bossier, P., Ekasari, J., 2017. Biofloc technology application in aquaculture to support sustainable development goals. Microb. Biotechnol. 10 (5), 1012–1016. https://doi.org/10.1111/1751-7915.12836.

Boyd, C.E., Tucker, C., McNevin, A., Bostick, K., Clay, J., 2007. Indicators of resource use efficiency and environmental performance in fish and crustacean aquaculture. Rev. Fish. Sci. 15, 327–360. https://doi.org/10.1080/10641260701624177.

Daigger, G.T., 2011. A practitioner's perspective on the uses and future developments for wastewater treatment modelling. Water Sci. Technol. 63 (3), 516–526. https://doi.org/10.2166/wst.2011.252.

Davis, T.L., Dirks, B., Carnero, E.A., Corbin, K.D., Krakoff, J., Parrington, S., Lee, D., Smith, S.R., Rittman, B.E., Krajmalnik-Brown, R., Marcus, A.K., 2021. Chemical oxygen demand can be converted to gross energy for food items using a linear regression model. J. Nutr. 151 (2), 445–453. https://doi.org/10.1093/jn/nxaa321.

de Korte, M., Bergman, J., van Willigenburg, L.G., Keesman, K.J., 2024. Towards a zero-waste aquaponics-centered eco-industrial food park. J. Clean. Prod. 454, 142109. https://doi.org/10.1016/j.jclepro.2024.142109.

De Schryver, P., Crab, R., Defoirdt, T., Boon, N., Verstraete, W., 2008. The basics of bio-flocs technology: the added value for aquaculture. Aquaculture 277 (3-4), 125–137. https://doi.org/10.1016/j.aquaculture.2008.02.019.

Ebeling, J.M., Timmons, M.B., Bisogni, J.J., 2006. Engineering analysis of the stoichiometry of photoautotrophic, autotrophic, and heterotrophic removal of ammonia-nitrogen in aquaculture systems. Aquaculture 257, 346–358. https://doi.org/10.1016/j.aquaculture.2006.03.019.

Ekasari, J., Azhar, M.H., Surawidjaja, E.H., Nuryati, S., De Schryver, P., Bossier, P., 2014. Immune response and disease resistance of shrimp fed biofloc grown on different carbon sources. Fish. Shellfish Immunol. 41 (2), 332–339. https://doi.org/10.1016/j.fsi.2014.09.004.

FAO, 2024. FishStat: Glob. Prod. Prod. Source 1950–2022 (www.fao.org/fishery/en/statistics/software/fishstatj).

Goddek, S., Espinal, C.A., Delaide, B., Jijakli, M.H., Schmautz, Z., Wuertz, S., Keesman, K. J., 2016. Navigating towards decoupled aquaponic systems: a system dynamics design approach. Water 8 (7), 303. https://doi.org/10.3390/w8070303.

Henze, M., Grady Jr, C.L., Gujer, W., Marais, G.V.R., Matsuo, T., 1987. A general model for single-sludge wastewater treatment systems. Water Res. 21 (5), 505–515. https://doi.org/10.1016/0043-1354(87)90058-3.

Jiménez-Montealegre, R., Verdegem, M.C.J., Van Dam, A., Verreth, J.A.J., 2002. Conceptualization and validation of a dynamic model for the simulation of nitrogen transformations and fluxes in fish ponds. Ecol. Model. 147 (2), 123–152. https://doi.org/10.1016/S0304-3800(01)00403-3.

Kabir, K.A., Verdegem, M.C.J., Verreth, J.A.J., Phillips, M.J., Schrama, J.W., 2020. Dietary non-starch polysaccharides influenced natural food web and fish production in semi-intensive pond culture of Nile tilapia. Aquaculture 528, 735506. https://doi.org/10.1016/j.aquaculture.2020.735506.

Keesman, K.J., 2011. System identification: an introduction. Springer Science & Business Media.

Li, X., Lei, S., Wu, G., Yu, Q., Xu, K., Ren, H., Wang, Y., Geng, J., 2023. Prediction of pharmaceuticals removal in activated sludge system under different operational parameters using an extended ASM-PhACs model. Sci. Total Environ. 871, 162065. https://doi.org/10.1016/j.scitotenv.2023.162065.

Mohammadi, F., Bina, B., Rahimi, S., Janati, M., 2022. Modelling of micropollutant fate in hybrid growth systems: model concepts, Peterson matrix, and application to a lab-scale pilot plant. Environ. Sci. Pollut. Res. 29 (45), 68707–68723. https://doi.org/10.1007/s11356-022-20668-2.

Muller, M. S., & Bauer, C. F. (1994). *Oxygen consumption of Tilapia and preliminary mass flows through a prototype closed aquaculture system* (No. NASA-TM-111882).

Pinho, S.M., de Lima, J.P., Tarigan, N.B., David, L.H., Portella, M.C., Keesman, K.J., 2023. Modelling FLOCponics systems: Towards improved water and nitrogen use efficiency in biofloc-based fish culture. Biosyst. Eng. 229, 96–115. https://doi.org/10.1016/j.biosystemseng.2023.03.022.

Ribeiro, J.M., Conca, V., Santos, J.M., Dias, D.F., Sayi-Ucar, N., Frison, N., Oehmen, A., 2022. Expanding ASM models towards integrated processes for short-cut nitrogen removal and bioplastic recovery. Sci. Total Environ. 821, 153492. https://doi.org/10.1016/j.scitotenv.2022.15349.

Schveitzer, R., Arantes, R., Costódio, P.F.S., do Espírito Santo, C.M., Arana, L.V., Seiffert, W.Q., Andreatta, E.R., 2013. Effect of different biofloc levels on microbial activity, water quality and performance of Litopenaeus vannamei in a tank system operated with no water exchange. Aquac. Eng. 56, 59–70. https://doi.org/10.1016/j.aquaeng.2013.04.006.

Serpa, D., Pousão-Ferreira, P., Caetano, M., da Fonseca, L.C., Dinis, M.T., Duarte, P., 2013. A coupled biogeochemical-Dynamic Energy Budget model as a tool for managing fish production ponds. Sci. Total Environ. 463, 861–874. https://doi.org/10.1016/j.scitotenv.2013.06.090.

Serra, F.P., Gaona, C.A., Furtado, P.S., Poersch, L.H., Wasielesky, W., 2015. Use of different carbon sources for the biofloc system adopted during the nursery and grow-out culture of Litopenaeus vannamei. Aquac. Int. 23, 1325–1339. https://doi.org/10.1007/s10499-015-9887-6.

Snip, L., 2010. Quantifying the greenhouse gas emissions of wastewater treatment plants [MSc Thesis. Wageningen University & Research]. Wageningen University & Research Library. https://edepot.wur.nl/138115.

Stanley, J.G., Jones, J.B., 1976. Feeding algae to fish. Aquaculture 7 (3), 219–223. https://doi.org/10.1016/0044-8486(76)90140-X.

Svirezhev, Y.M., Krysanova, V.P., Voinov, A.A., 1984. Mathematical modelling of a fish pond ecosystem. Ecol. Model. 21 (4), 315–337. https://doi.org/10.1016/0304-3800(84)90066-8.

Tarigan, N.B., Amal, M.J. r, Ekasari, J., Keesman, K.J., Verdegem, M., 2025. Nitrogen, phosphorus, and carbon dynamics in biofloc system of Nile tilapia fed with high non-starch polysaccharides diet. Aquaculture 596. https://doi.org/10.1016/j.aquaculture.2024.741714.

Tarigan, N.B., Goddek, S., Keesman, K.J., 2021. Explorative study of aquaponics systems in Indonesia. Sustainability 13 (22), 12685. https://doi.org/10.3390/su132212685.

Tarigan, N.B., Verdegem, M., Ekasari, J., Keesman, K.J., 2024. Nutrient flows in biofloc-Nile tilapia culture: A semi-physical modelling approach. Biosyst. Eng. 248, 108–129. https://doi.org/10.1016/j.biosystemseng.2024.09.021.

Tinh, T.H., Momoh, T.A., Kokou, F., Hai, T.N., Schrama, J.W., Verreth, J.A., Verdegem, M.C., 2021. Effects of carbohydrate addition methods on Pacific white shrimp (*Litopenaeus vannamei*). Aquaculture 543, 736890. https://doi.org/10.1016/j.aquaculture.2021.736890.

Verdegem, M., Buschmann, A.H., Latt, U.W., Dalsgaard, A.J., Lovatelli, A., 2023. The contribution of aquaculture systems to global aquaculture production. J. World Aquac. Soc. 54 (2), 206–250. https://doi.org/10.1111/jwas.12963.

Vinasyiam, A., Kokou, F., Ekasari, J., Schrama, J.W., Verdegem, M.C., 2023. Effects of high wheat bran input on the performance of a biofloc system for Pacific white shrimp (*Litopenaeus vannamei*). Aquac. Rep. 33, 101853.

Wolfe, J.R., Zweig, R.D., Engstrom, D.G., 1986. A computer simulation model of the solar-algae pond ecosystem. Ecological modelling 34 (1–2), 1–59. https://doi.org/10.1016/0304-3800(86)90078-5.